

# GOLD NANOPARTICLES PAPER AS SURFACE ENHANCED RAMAN SCATTERING (SERS) PLATFORM FOR BIO-DIAGNOSTIC APPLICATIONS

*Ying Hui Ngo, Whui Lyn Then and Gil Garnier*

BioPRIA, Australian Pulp and Paper Institute (APPI), Department of Chemical Engineering, Monash University, Clayton, VIC 3800, Australia.

## ABSTRACT

We explored the sensitivity and selectivity of gold nanoparticles (AuNPs) treated paper as a generic SERS diagnostic platform to identify and quantify low concentrations of a specific (bio)analyte in aqueous solutions. The effects of gold nanoparticles (AuNPs) concentration on their adsorption and aggregation states on paper were explored. The surface coverage of AuNPs on paper scaled linearly with their concentration profile in solutions. The SERS performances of the AuNPs-treated papers were evaluated with a model Raman molecule, 4-aminothiophenol (4-ATP), and their SERS intensities increased linearly with the density of AuNPs on paper. To increase the SERS sensitivity, the retention and aggregation state of nanoparticles on paper was controlled by pre-treating paper with a series of cationic polyacrylamide (CPAM) solutions. The CPAM pre-treated paper produced a more uniform distribution of AuNPs compared to untreated paper. Higher surface coverage and aggregation of AuNPs on paper were favoured by CPAM solutions of higher concentration,

charge density and molecular weight. The optimized AuNPs-CPAM paper showed a higher sensitivity and Raman enhancement factor (EF), which was almost an order of magnitude higher than the untreated AuNPs paper. After the SERS sensitivity towards the detection of model Raman molecule (4-ATP) was proven, the SERS selectivity of AuNPs paper was demonstrated by functionalizing the AuNPs with a model biomolecule platform consisting of biotin/streptavidin assemblies for the detection of antibody-antigen binding. The modification of antibody local structure due to the interaction with antigen was detected. Evidence of antigen binding was elucidated from the SERS spectra, confirming the presence of antigen. Reproducible spectra features were observed for the functionalized AuNP papers which were exposed to different concentration of antigen; the spectra intensity increased as a function of antigen concentration. The sensitivity and selectivity of AuNPs paper substrates as a low-cost and generic SERS platform for bio-diagnostic application was demonstrated.

**Keywords:** Gold nanoparticles (AuNPs), paper, Surface Enhanced Raman Scattering (SERS), Cationic Polyacrylamide (CPAM), 4-aminothiophenol (4-ATP), antibody, antigen, biotin, streptavidin.

## 1 INTRODUCTION

Paper has emerged as an efficient substrate in the fabrication of low-cost diagnostics for medical and environmental applications [1–2]. A full review of bioactive paper was provided by Pelton et al. [3] and by Then and Garnier [4]. Among the developing applications is bioactive paper diagnostic for blood typing, wherein blood agglutination is triggered by specific antibody-antigen interactions and indicated by chromatographic separation on paper [1–2, 5]. However, bioactive papers often suffer from four major issues: Specificity, Selectivity, Sensitivity and Simplicity (4S). Paper tests rely mostly on colorimetric technique to communicate the result of analysis. Although direct and convenient, the sensitivity of colorimetric techniques on paper is usually limited to the  $10^{-6}$  M range. For certain applications, such as early cancer detection, a micro-molar sensitivity can be insufficient and a detection ranging between  $10^{-9}$  to  $10^{-12}$  M might be needed. An amplification technique is therefore required to increase the detection range by 3 to 6 orders of magnitude. The challenge is to increase sensitivity and selectivity without compromising cost and ease of use. While Enzyme-linked immunosorbent assay (ELISA) has become a standard in biomedical science, its applica-

tion to paper and low cost diagnostics is cumbersome. ELISA is a standard solution-based technique which can be used to identify and quantify analyte (usually antibodies or antigens) by colour indication; it requires multiple reactants and washing steps. A more attractive option is Surface Enhanced Raman Scattering (SERS) technology which allows single molecule detection [6]. With the commercial availability of low-cost field-portable Raman spectrometers, SERS seems ideal for bio-diagnostic applications. Raman spectroscopy involves non-destructive and non-contact method of obtaining instant fingerprint spectrum of materials and no requirement for special sample preparation. Metal aqueous colloids were among the first conventional SERS substrates. Unfortunately, their application has been challenged by low reproducibility and stability. This has led to the development of techniques to immobilize metallic nanoparticles on solid substrates such as glass and silicon. However, these techniques are time consuming, costly, require sophisticated equipment to manufacture the test, and the resulting substrates are often fragile and suffer from poor storage stability. Paper has emerged as an efficient substrate for routine SERS analysis due to its robustness, low-cost, wide availability and ability to be engineered. The combination of functionalized AuNP treated paper with the hand held Raman spectrometers opens new horizons for low-cost field biodiagnostics. However, there is a poor understanding of the role played by paper in this SERS biodiagnostic application.

This article reports the development of gold nanoparticles (AuNPs) paper as a generic platform for biodiagnostics. AuNPs paper can be used as a standard substrate that directly contacts a fluid of the body, followed by rapid Surface Enhanced Raman Scattering (SERS) molecular detection to identify and quantify the analyte of interest [7]. Detection selectivity is insured by two processes. First, by the Raman spectra molecularly specificity; second, by a molecule immobilized on the nanoparticle (such as an antigen) which is affinity specific to the analyte of interest (such as an antibody). In our study, AuNP paper was simply prepared by dipping filter paper in AuNPs suspensions of increasing concentrations. Paper pre-treatment with cationic polyacrylamide (CPAM) was investigated to improve sensitivity and retention of AuNPs [8]. The enhancement factor (EF) of Raman scattering is known to be drastically affected by the concentration of “hot spots” typically formed by NP-NP contact, and therefore affected by the AuNP aggregate size and surface coverage on paper. A standard Raman molecule, 4-aminothiophenol (4-ATP), was used as analyte model in this study. We then investigated the functionalization of preformed gold nanoparticle (AuNP) aggregates on paper with antigens and various biomolecules by taking advantage of the strong thiol-gold interaction to functionalise AuNPs with model biomolecules. We relied on the high affinity association between the *Streptomyces avidinii*-derived protein, streptavidin, and biotin for selective biorecognition. The binding

interaction of the antibody with its specific antigen was detected using SERS. It is the objective of the study to critically analyse the potential of AuNP treated paper as a generic platform for low cost biodiagnostics.

## **2 EXPERIMENTAL SECTION**

### **2.1 Materials**

Hydrogen tetrachloroaurate trihydrate ( $\text{HAuCl}_4 \cdot 3\text{H}_2\text{O}$ ) and sodium citrate tribasic dihydrate ( $\text{Na}_3\text{C}_6\text{H}_5\text{O}_7 \cdot 2\text{H}_2\text{O}$ ) were purchased from Sigma-Aldrich and used as received. Whatman qualitative filter paper #1, which consists of 98%  $\alpha$ -cellulose, was selected as the paper substrate as it is a convenient model paper of well-defined structure and to ensure minimal SERS interference from process components (polymers or coatings). The cationic trimethylaminoethyl-methacrylate polyacrylamide (CPAM) polymers were supplied by AQUA+TECH Switzerland from their SnowFlake Cationics product range, and used as received (chemical structure shown in Supporting Information, S1). They were identified as: I1 (5 wt% charge density, molecular weight 13 MDa), H1 (10 wt% charge density, molecular weight 13 MDa), F1 (40 wt% charge density, molecular weight 13 MDa) and F3 (40 wt % charge density, molecular weight 6 MDa). Biotinylated polyethylene glycol (PEG) thiol was purchased from Nanocs, Wisconsin, USA. Triethylene glycol mono-11-mercaptoundecyl ether (TEG) and recombinant streptavidin lyophilized powder was purchased from Sigma-Aldrich. Anti-rabbit IgG-biotin and rabbit IgG were purchased from Protein Mods, New York, USA.

### **2.2 Fabrication of AuNPs treated Paper**

AuNPs were synthesized by using 1 mM  $\text{HAuCl}_4 \cdot 3\text{H}_2\text{O}$  and 1% aqueous  $\text{Na}_3\text{C}_6\text{H}_5\text{O}_7 \cdot 2\text{H}_2\text{O}$  according to the Turkevich method [9]. A stock solution of CPAM was prepared on the day of the experiment by diluting dry powder to 0.1 mg/mL with Millipore water, and gently mixing the dispersions for 8 hours at 23°C to facilitate the dissolution process. Filter papers (55 mm diameter) were used as received, or were pretreated with the cationic polymer. For treatment, the filter papers were dipped into 10 mL polymer solutions for 1 hour, rendering the paper cationic. The treated papers were rinsed with distilled water to remove any unbounded polymer. Wet pieces of untreated and polymer-treated paper substrates were then dipped immediately into Petri dishes containing 10 mL solution of AuNPs for 24 hours. After dipping, the paper substrates were rinsed thoroughly with distilled water to remove any loosely bound AuNPs, and the papers were air-dried and stored at 50% relative humidity and 23°C until further analysis.

### 2.3 SERS sensitivity

Solutions of 1 mM of 4-ATP were prepared in ethanol. 4-ATP is known for its strong affinity to the surface of AuNPs (its S-H bond is easily cleaved to form Au-S bond upon adsorption). In order to study their SERS sensitivity, the dried AuNPs-treated substrates were dipped into 2 mL of 4-ATP ethanol solution for 5 minutes to obtain a monolayer of 4-ATP on the substrates. After thorough rinsing with ethanol and drying, they were subjected to Raman characterization. Raman enhancement factor (EF) of 1 mM of 4-ATP on a substrate was calculated as follow [10–11]:

$$EF = \frac{[I_{SERS}]}{[I_{bulk}]} \times \frac{[N_{bulk}]}{[N_{ads}]} \quad (1)$$

where  $I_{SERS}$  is the intensity of a specific band in the SERS spectrum of 4-ATP and  $I_{bulk}$  is the intensity of the same band in the Raman spectrum from the bulk solution sample. For all spectra, the intensity of the band at  $1077 \text{ cm}^{-1}$  was used to calculate EF values.  $N_{bulk}$  is the number of molecules of the bulk 4-ATP in the laser illumination volume while  $N_{ads}$  is the number of molecules adsorbed and sampled on the SERS active substrate within the laser spot.

### 2.4 SERS selectivity

The dried AuNPs papers were immersed in an ethanol solution for 30 min. They were then immersed into a  $5 \times 10^{-4} \text{ M}$  TEG (blocking thiol) and  $5 \times 10^{-4} \text{ M}$  BAT (biotinylated thiol) solution (9:1 ratio) for 6 hours (Figure 1b). After drying, the samples were immersed into a  $5 \times 10^{-7} \text{ M}$  Streptavidin solution in PBS for 2 hours (Figure 1c). After rinsing with a PBS solution, the samples were dipped in a 0.1 M antibody solution for 30 min (Figure 1d). The functionalization step was completed by dipping the dried samples in a 0.1 M antigen solution for 60 min (Figure 1e). All solution treatments were at room temperature ( $22 \text{ }^\circ\text{C}$ ).

**Table 1.** Size or molecular weight of each component

<i>Component</i>	<i>Size/molecular weight</i>
AuNPs	23.2 nm
TEG	376.53 Da
BAT	5 kDa
Strep	75 kDa
Biotinylated Antibody	150 kDa
Antigen	8–10 kDa

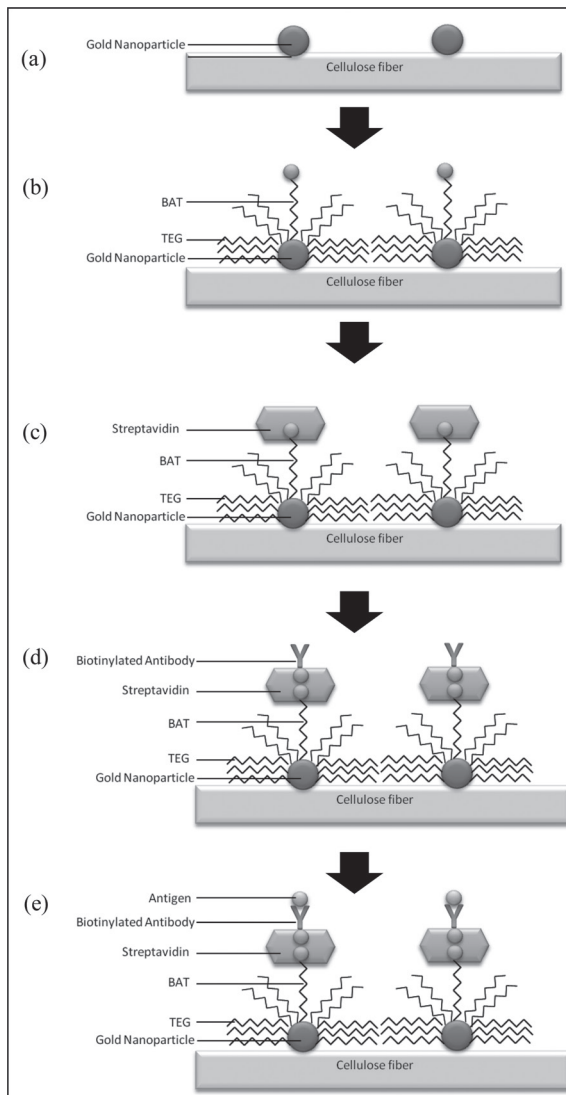


**Figure 1.** Functionalization procedure of AuNPs paper as a SERS platform.

## **2.5 Instrumentation**

Field Emission Scanning Electron Microscopy (FESEM), which produces higher resolution, less sample charging and less damaged images than conventional SEM, was performed using a JEOL 7001 Field Emission Gun (FEG) system operating at 5 kV and 180 pA. ImageJ analysis software was used to determine the coverage of AuNPs on the cellulose fibers in the FESEM images and estimate the particle size distribution. All Raman and SERS spectra were obtained in air using a Renishaw Invia Raman microscope equipped with a 300 mW 633 nm laser. The laser beam was positioned through a Leica imaging microscope objective lens (50×), whilst the instrument's wavenumber was calibrated with a silicon standard centered at 520.5  $\text{cm}^{-1}$  shift. Due to the smaller spot size of the laser compared with the large surface area of the samples, the spectra were obtained at 5 different points of the surface. The average Raman intensity (of 5 measurements) was presented as the final result after baseline subtraction from the control samples.

## **3 RESULTS AND DISCUSSION**

### **3.1 SERS sensitivity**

#### *3.1.1 AuNPs paper*

A stock solution of 0.20 mg/mL of AuNPs was synthesized using the Turkevich method [9]. Particle size measurement by Dynamic Light Scattering (DLS) revealed a highly monodispersed AuNPs suspension with an average diameter of 23.2 nm. AuNPs suspensions of different concentrations (0.15 mg/mL, 0.10 mg/mL, 0.05 mg/mL, 0.02 mg/mL) were prepared by diluting the stock solution (0.20 mg/mL). The diameter of the AuNPs can be varied by adjusting the concentration ratio between the gold salt and the reducing citrate solution; the diameter of AuNPs was kept constant in this work.

Filter paper samples were dipped into the AuNP solutions for 24 hours. This procedure aimed at keeping the size of AuNPs retained on paper constant. The colour intensity of the dried AuNPs treated papers was analysed with ImageJ software (Figure 2). AuNPs treated paper turned from white to red purple and the colour became more intense as the concentration of AuNP solutions was increased.

FESEM images (Figure 3) were also analysed using ImageJ software to measure the quantity and size distribution of AuNPs adsorbed on paper. The size distribution of AuNP remained constant for all experiments with an average size of  $25 \pm 3$  nm; this means that most AuNPs are retained on paper as individual particles. The total number of AuNPs was estimated by dividing the total area of

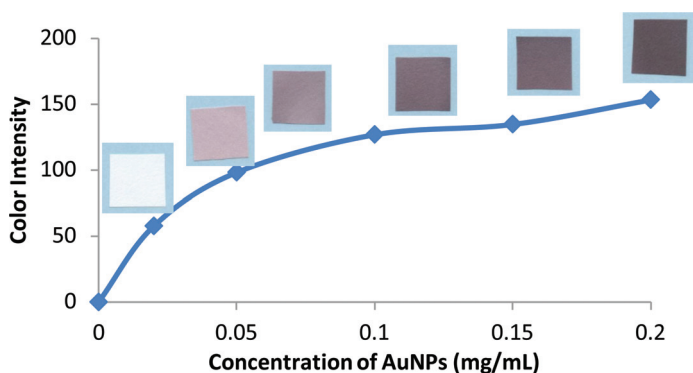


**Figure 2.** Colour intensity of filter papers treated with AuNP solutions of different concentrations.

AuNPs on paper (in each FESEM images) by the area of an individual AuNP ( $d=23.2$  nm). The concentration of AuNPs on paper increased monotonically with the solution concentration in which the papers were dipped in; the particle distribution was denser and more uniform on paper when treated with AuNP solutions of higher concentration. The average distance between the AuNPs decreased from 100–200 nm to 10–50 nm, as observed from paper treated with the lowest to the highest concentration of AuNP suspension, respectively (Figure 3).

4-Aminothiophenol (4-ATP) was selected as the probe molecule in the Raman analysis because of its distinct Raman features, strong affinity for metal surfaces via thiol bonding and the formation of self-assembled monolayers [12]. Control paper and AuNP treated papers were dipped into 1 mM of 4-ATP for 5 minutes, washed, dried and analysed by Raman spectroscopy. The concentration effect of AuNP solutions on the SERS signal from paper substrates was quantified (Figure 4). All spectra exhibited similar peak positions and relative height; only the intensity of the spectra varied. The spectra were dominated by three strong bands:  $\delta(\text{C-S})$  at  $387\text{ cm}^{-1}$ ,  $\nu(\text{C-S})$  at  $1077\text{ cm}^{-1}$  and  $\nu(\text{C-C})$  at  $1584\text{ cm}^{-1}$ , which were the  $a_1$  vibrational modes (in-plane, in-phase modes) of the 4-ATP molecules [13]. The significant enhancement of  $a_1$  modes was related to the enhancement of the electromagnetic field between the AuNPs, which was produced by the strong inter-nanoparticles coupling among the close contacted AuNPs. Notably, the  $b_2$  bending modes (in-plane, out-of-phase modes) were  $\delta(\text{C-H})$  at  $1137\text{ cm}^{-1}$ ,  $\delta(\text{C-H}) + \nu(\text{C-C})$  at  $1386\text{ cm}^{-1}$  and  $\delta(\text{C-H}) + \nu(\text{C-C})$  at  $1433\text{ cm}^{-1}$  [13]. The significant enhancement of  $b_2$  modes may be attributed to the

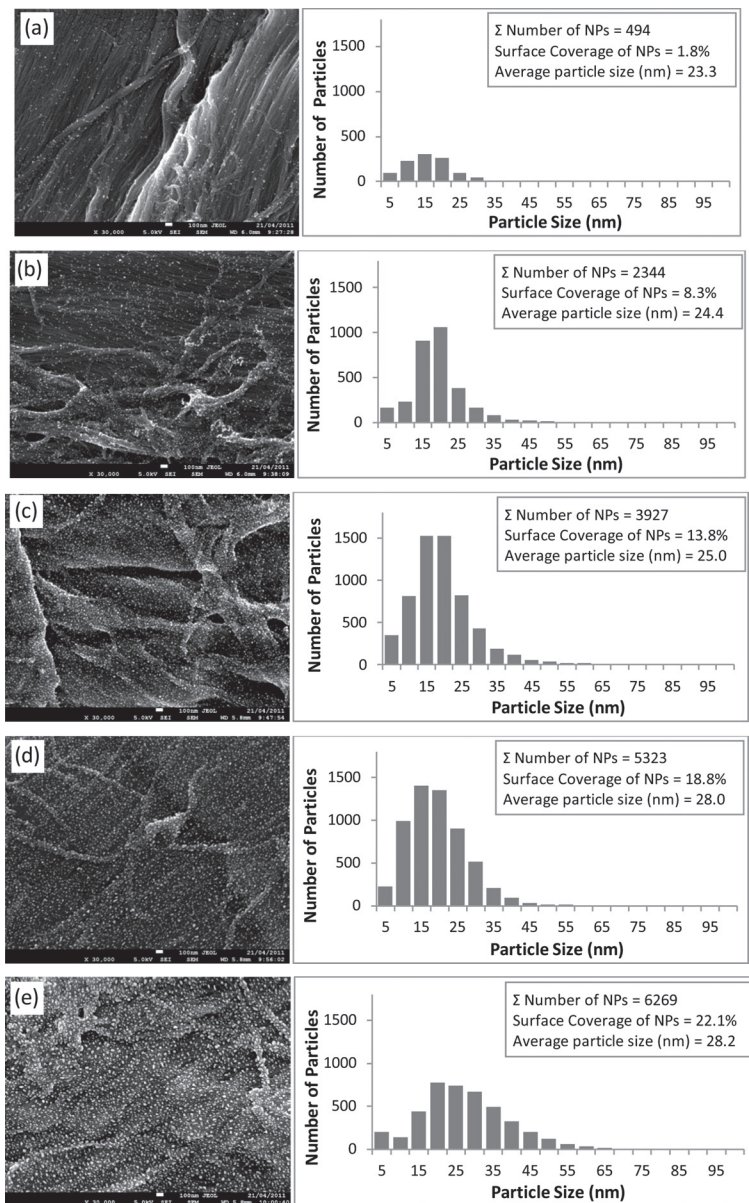


**Figure 3.** FESEM images and histograms of particle size distribution of filter papers dipped into (a) 0.02 mg/mL, (b) 0.05 mg/mL, (c) 0.10 mg/mL, (d) 0.15 mg/mL and (e) 0.20 mg/mL of AuNP solutions.

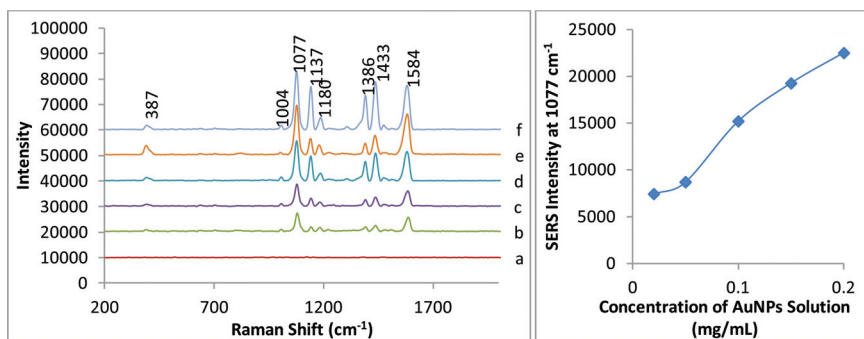


**Figure 4.** (Left) Raman spectrum of 1 mM of 4-ATP adsorb on (a) plain filter paper and SERS spectra of 4-ATP on filter paper dipped in AuNP solutions of (b) 0.02 mg/mL, (c) 0.05 mg/mL, (d) 0.10 mg/mL, (e) 0.15 mg/mL and (f) 0.20 mg/mL. (Right) SERS intensity of 4-ATP at 1077  $\text{cm}^{-1}$  band from paper dipped in different concentration of AuNP solutions.

charge transfer of AuNPs to the absorbed 4-ATP molecules which was largely dependent on the energy of the excitation laser.

The SERS potential of AuNP treated papers was demonstrated by the drastic increase in intensities. Treating paper with 0.02 mg/mL of AuNPs significantly enhanced the Raman signal of 4-ATP (Figure 4a and 4b). The SERS intensity of AuNPs-treated paper was found to increase linearly with the concentration of AuNP solutions applied to paper (Figure 4). As the AuNP concentration in solution increased, the interparticle distance decreases; the AuNP retained their packing density once adsorbed onto paper. As the average distance between the AuNPs decreased from approximately 100–200 nm to 10–50 nm, effective ‘hot spots’ appeared and their interparticle plasmon coupling gave rise to the enhancement of electromagnetic field which intensified the SERS signals of 4-ATP [14]. This significant SERS signal enhancement was particularly observed for paper treated with AuNPs concentration of 1.0 mg/mL (Figure 4) as the interparticle distance of the AuNPs became similar to their diameter ( $25 \pm 3$  nm).

### 3.1.2 AuNPs-CPAM paper

A higher SERS efficiency is expected from aggregates than from individual nanoparticles because of the greater SERS enhancement at their contact points [15]. To test this hypothesis, filter paper samples were pre-treated with CPAM solutions of different concentrations. A high molecular weight (13 MDa) and highly charged (40 wt%) CPAM was selected. This was to induce a positive charge on paper

(originally negatively charged) and to create a polymer layer able to adsorb, retain and aggregate the negatively charged AuNPs. The positive charge of the CPAM solutions increased with their polymer concentration, as measured by their zeta potential. After CPAM pre-treatment, the filter papers were thoroughly rinsed and directly dipped into a 0.20 mg/mL AuNPs solution for 24 hours.

The colour intensity of the dried AuNPs and AuNPs-CPAM treated papers was analysed with ImageJ software (Figure 5). The colour of the paper turned from reddish-purple (AuNPs on untreated paper) to dark purple when the paper was pre-treated with CPAM, followed by AuNPs; the colour became darker as the concentration of CPAM was increased.

FESEM analysis was performed to examine the adsorption of AuNPs on the untreated and CPAM pre-treated papers. Pre-treating paper with the dilute 0.01 mg/mL CPAM did not increase AuNP aggregate size but more than doubled the AuNP surface coverage on paper (Figures 6a and 6b). As the concentration of CPAM solution was increased, the assembly of AuNPs was drawn together, forming a random distribution of two- and three-dimensional clusters within the paper micro-structure (Figure 6). The surface coverage and size of AuNPs aggregates also increased dramatically to 84.6% and 59.6 nm, respectively, for paper pre-treated with the concentrated CPAM solution (0.10 mg/mL) (Figure 6e).

The concentration effect of CPAM solutions on the SERS signal of 4-ATP from AuNPs treated paper substrates was quantified (Figure 7). The Raman

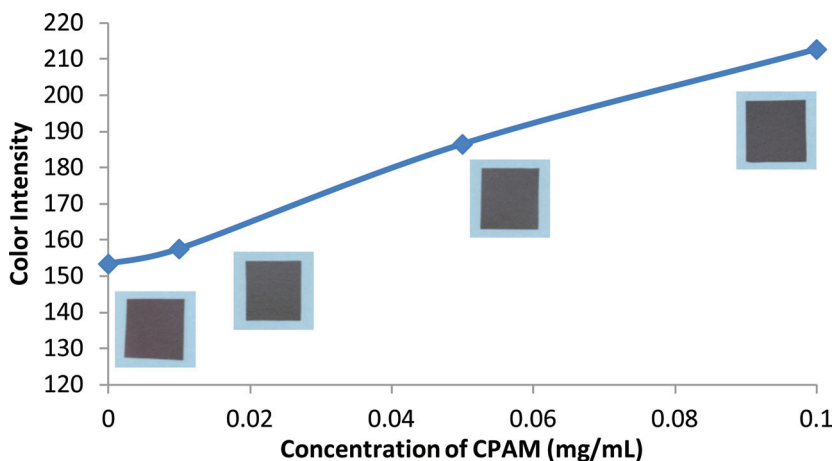


**Figure 5.** Colour intensity of filter paper dipped in 0.20 mg/mL of AuNP solutions without CPAM pre-treatment and with CPAM pre-treatment of 0.01 mg/mL, 0.05 mg/mL and 0.10 mg/mL polymer concentration.

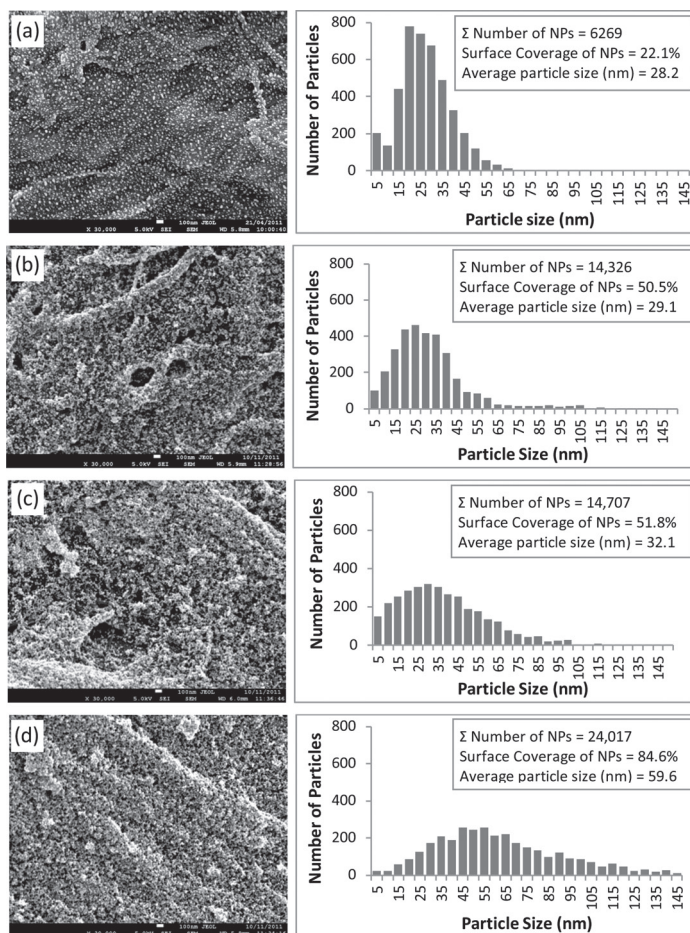


**Figure 6.** FESEM images and histograms of AuNP aggregate size distribution of filter paper dipped in 0.20 mg/mL of AuNP solutions (a) without CPAM pre-treatment and with CPAM pre-treatment of (b) 0.01 mg/mL (c) 0.05 mg/mL and (d) 0.10 mg/mL polymer concentration.

Enhancement Factor (EF) of 4-ATP doubled when paper was pre-treated with 0.01 mg/mL of CPAM. The Raman Enhancement Factor (EF) increased pseudo-linearly with the concentration of CPAM used for paper pre-treatment.

To study the effect of polymer charge density, paper substrates were pre-treated with a series of solutions of CPAM (0.10 mg/mL) having a constant molecular

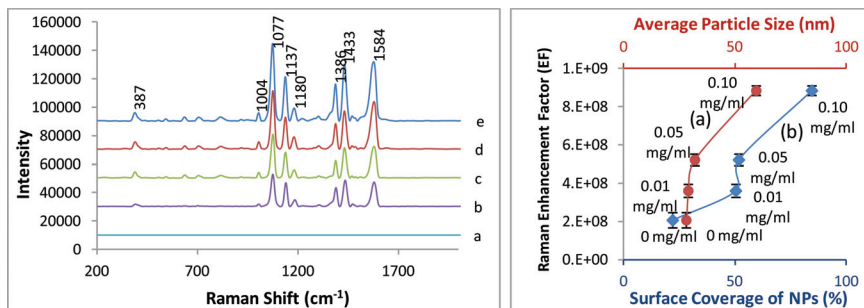


**Figure 7.** (Left) Raman spectrum of 4-ATP adsorbed on (a) plain filter paper, SERS spectra of 4-ATP on AuNPs paper (b) without CPAM pre-treatment and with CPAM pre-treatment of (c) 0.01 mg/ml (d) 0.05 mg/ml and (e) 0.10 mg/ml polymer's concentration. (Right) Relationship between the (a) average size and (b) surface coverage of AuNP aggregates and the EF of 4-ATP measured at the 1077 cm<sup>-1</sup> band (error bars show standard deviation of 5 measurements from different spots on the substrate).

weight (13MDa) but different charge densities; papers were then dipped into a 0.20 mg/mL AuNP solution. CPAM with a charge density of 5 wt%, 10 wt% and 40 wt% were tested. The surface coverage and average aggregate diameters of AuNPs increased from 62.2% to 84.6% and from 34.8 nm to 59.6 nm, respectively, as a function of the CPAM's charge density (Figure 8). The cluster size distribution also became wider. The charge density of the CPAM solution strongly affected the SERS enhancement of the AuNPs-CPAM paper (Figure 9). From an initial Raman EF of  $2.1 \times 10^8$ , the EF increased by a factor of 4 to  $8.9 \times 10^8$ .

The effect of CPAM's molecular weight on the aggregation and adsorption of AuNPs on paper was investigated. Paper was pre-treated with a lower molecular weight CPAM of 6 MDa (40 wt% charge density and 0.10 mg/mL concentration). The molecular weight of the CPAM strongly influenced the surface coverage and aggregation state of AuNPs. By doubling the CPAM molecular weight, the surface coverage and average diameter of AuNP aggregates increased, from 49% to 85% and 35nm to 60 nm, respectively (Figure 10). The Raman EF of AuNPs-CPAM paper was increased almost by a factor 3, from  $3.1 \times 10^8$  to  $8.9 \times 10^8$ , when paper was pre-treated with CPAM of higher molecular weight (Figure 11).

Filter paper pre-treated with a high concentration polymer solution, with a CPAM of high charge density and high molecular weight had a more uniform and denser distribution of AuNP aggregates. The increased proportion of aggregated AuNPs and the smaller interparticle spacing in CPAM-treated AuNP-deposited paper increased the coupling of Localized Surface Plasmon Resonances (LSPRs), which arise from the collective oscillation of electrons within metallic NPs [16].

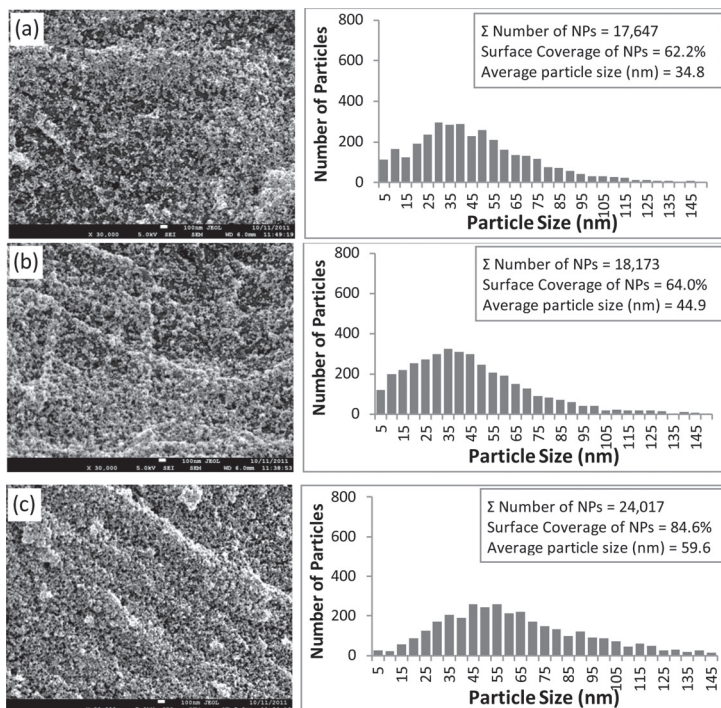


**Figure 8.** FESEM images and histograms of particle size distribution of AuNPs-CPAM papers treated with polymer solution charge density of (a) 5 wt%, (b) 10 wt% and (c) 40 wt%.

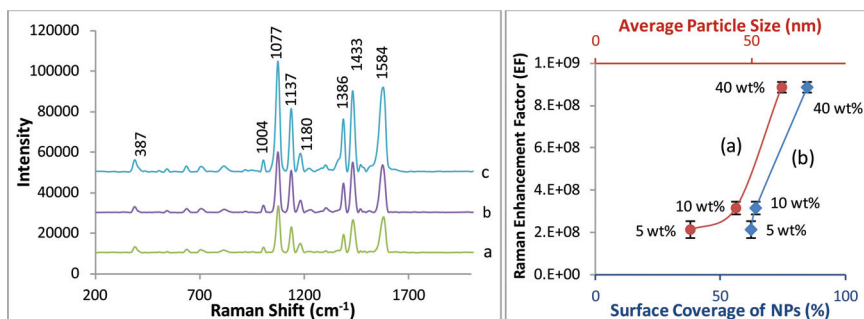


**Figure 9.** (Left) SERS spectra of 4-ATP on AuNPs-CPAM papers with polymer charge density of (a) 5 wt%, (b) 10 wt% and (c) 40 wt%. (Right) Relationship between the (a) average size and (b) surface coverage of AuNP aggregates and the EF of 4-ATP measured at the 1077 cm<sup>-1</sup> band (error bars show standard deviation of 5 measurements from different spots on the substrate).

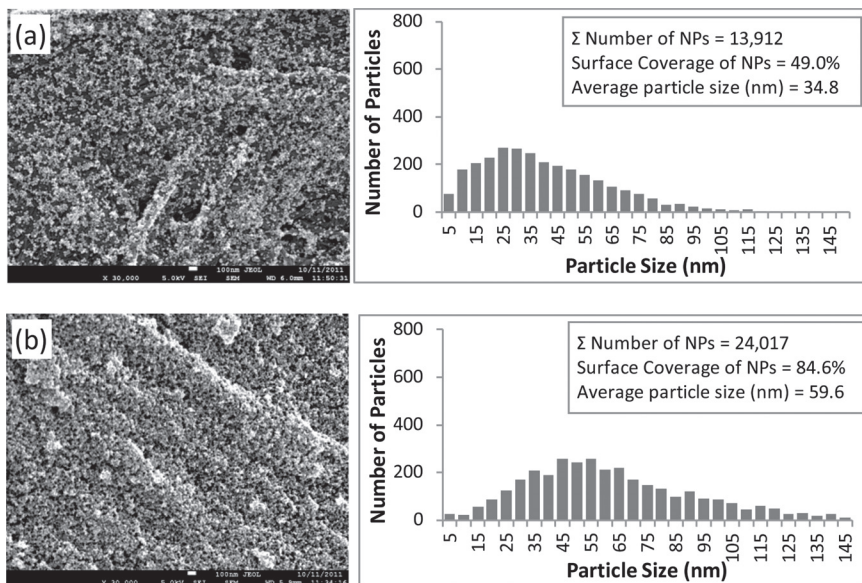


**Figure 10.** FESEM images and histograms of particle size distribution of AuNPs-CPAM papers with polymer molecular weight of (a) 6 MDa and (b) 13 MDa.

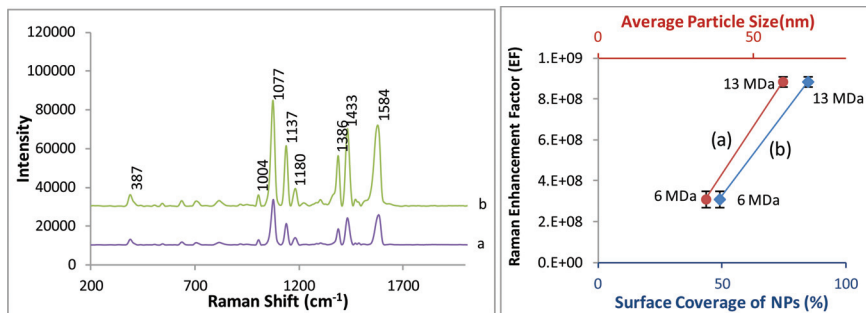


**Figure 11.** (Left) SERS spectra of 4-ATP on AuNPs-CPAM papers with polymer molecular weight of (a) 6 MDa and (b) 13 MDa. (Right) Relationship between the (a) average size and (b) surface coverage of AuNP aggregates and the EF of 4-ATP measured at the 1077 cm<sup>-1</sup> band (error bars show standard deviation of 5 measurements from different spots on the substrate).

This resulted in the formation of enhanced electromagnetic fields (hot spots), particularly at curved surfaces or gaps in between the AuNPs, thereby improving amplification of SERS signal. The SERS sensitivity of AuNPs-CPAM paper was quantified and compared with untreated AuNPs paper. Both untreated paper and paper pre-treated with CPAM (0.10 mg/mL, 13 MDa and 40 wt% charge density) were dipped into 0.20 mg/mL AuNP solutions, exposed to different concentrations of 4-ATP and their Raman spectra were measured (Figure 12 and Figure 13). The concentration of 4-ATP investigated ranged over 6 orders of magnitude, from 1 mM to 1 nM. Whilst the SERS spectra of 4-ATP for both papers were very

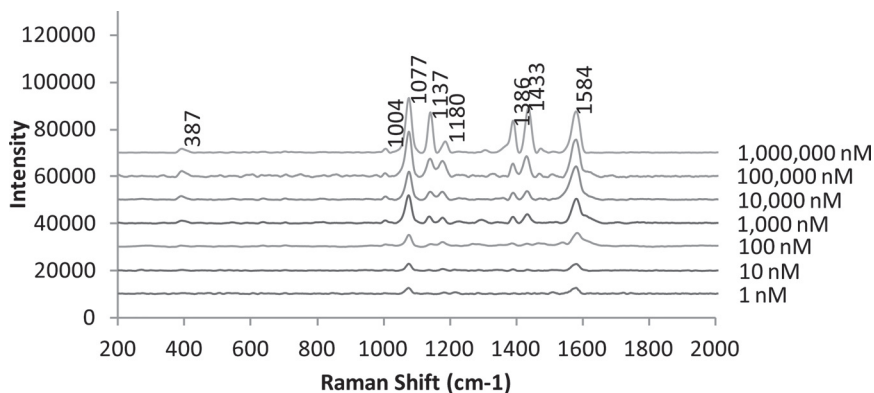


Figure 12. SERS spectra of different concentration of 4-ATP on AuNPs paper.

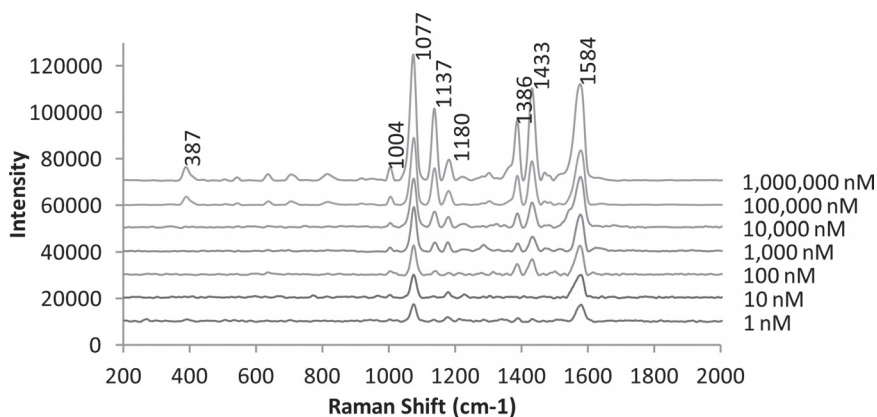
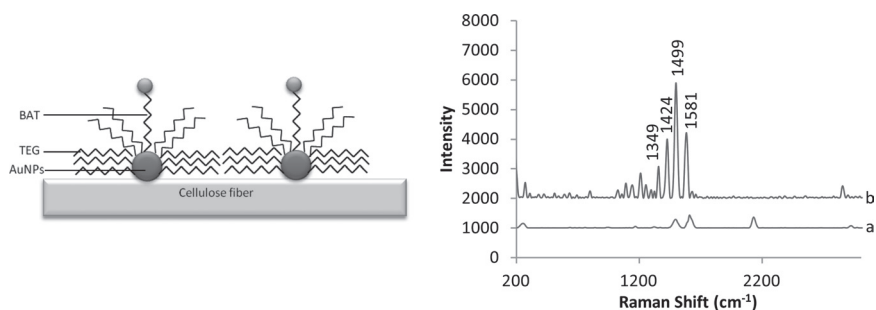


Figure 13. SERS spectra of different concentration of 4-ATP on AuNPs-CPAM paper.

similar, the SERS peaks were better defined on CPAM pre-treated paper. The detection limit of AuNPs-CPAM paper substrates was lower than for AuNPs on untreated paper as the spectrum of 1 nM of 4-ATP had good signal-to-noise ratio and the main peaks at  $1077\text{ cm}^{-1}$  and  $1584\text{ cm}^{-1}$  were more distinct. The Raman intensity of the AuNPs-paper pretreated with CPAM was doubled that of the untreated AuNP-paper over the entire range of 4-ATP concentration.

### 3.2 SERS Selectivity

In the first part of the study, the SERS sensitivity of AuNPs paper was optimized for the detection of a model Raman molecule (4-ATP). In this second part of the study, SERS sensitivity is studied with different biomolecules; this is achieved by functionalizing the AuNPs with biotin/streptavidin assemblies for the selective detection of antibody-antigen binding (Figure 1). Streptavidin/biotin assemblies were selected to functionalize the AuNPs for antibody-antigen detection since they are a well-known model system for molecular recognition and biorecognition and because of their stable bio-structure. The strong affinity of both molecules is based on the intra- and intermolecular interactions between tryptophan (Trp) residues and the non-polar side chain of streptavidin with the non-polar moieties of biotin [17]. To functionalize the AuNPs adsorbed on paper, a mixture of biotinylated alkane thiol (BAT) and alkane thiol (TEG) was first adsorbed on the AuNPs via the strong affinity Au-S bonding. Due to the large structure of Streptavidin, it is necessary to use a blocking thiol molecule (TEG) to block the unbound sites of AuNPs between the BAT molecules. This prevents the nonspecific binding of other molecular compounds to the surface of AuNPs. Figure 14 shows the corresponding SERS spectra before and after the AuNPs paper was treated with the thiol mixture. The SERS spectrum (b) shows a strong characteristic SERS



**Figure 14.** Left: Schematic diagram of BAT/TEG functionalized AuNPs on paper. Right: SERS spectra of (a) AuNPs paper and (b) BAT/TEG functionalized AuNPs paper.

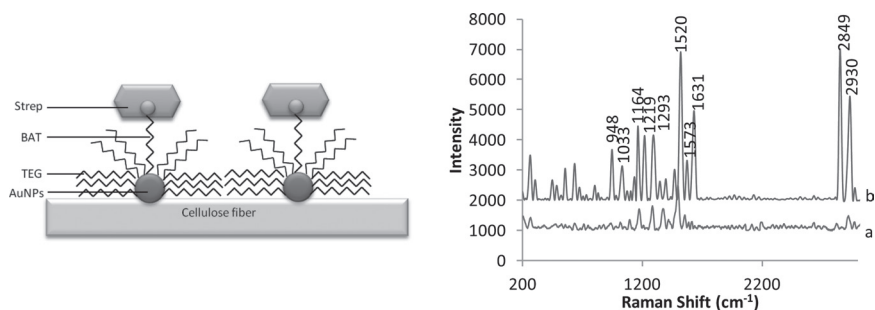


**Figure 15.** Left: Schematic diagram of Strep-BAT/TEG functionalized AuNPs on paper. Right: SERS spectra of (a) Streptavidin on AuNPs paper and (b) Strep-BAT/TEG functionalized AuNPs paper.

band of BAT and TEG on AuNPs paper compared to the untreated AuNPs paper (spectrum a), confirming the successful binding of the thiol mixture. The spectrum was dominated by four strong characteristic bands:  $\omega(\text{CH}_2)$  at  $1349\text{ cm}^{-1}$ ,  $\text{Bio}/\nu(\text{CH}_2)$  ring at  $1424\text{ cm}^{-1}$  and  $1499\text{ cm}^{-1}$  and  $\nu(\text{C-N})$  at  $1581\text{ cm}^{-1}$  [17].

Streptavidin was then bound onto the biotinylated thiol. A significantly different SERS spectrum (Figure 15) resulted, confirming the successful binding of streptavidin. All SERS spectra are plotted with the same scales for easy comparison (Figures 14–17). The resulting spectrum was dominated by Trp16 observed at  $948\text{ cm}^{-1}$ , Phe, Ser at  $1033\text{ cm}^{-1}$ ,  $\nu(\text{C-N})$ , Trp13 at  $1164\text{ cm}^{-1}$ , amide III ( $\beta$  sheet) at  $1219\text{ cm}^{-1}$ ,  $\omega(\text{CH}_2)$  at  $1293\text{ cm}^{-1}$ , Trp3 at  $1520\text{ cm}^{-1}$ , Trp2 at  $1573\text{ cm}^{-1}$ , amide I ( $\beta$  sheet) at  $1631\text{ cm}^{-1}$  and  $\nu(\text{C-H})$  at  $2849\text{ cm}^{-1}$  to  $2930\text{ cm}^{-1}$  [17]. All the spectra of BAT/TEG and Streptavidin-BAT/TEG functionalized AuNPs papers were obtained from the average of five Raman measurements at different spots (Supporting Information, S2). The laser power was maintained at 10% and the exposure time was kept at 1 sec to prevent the biomolecule to denature. The position of all the characteristic bands was reproducible with little variation in intensity ( $\pm 10$ – $20\%$ ) (Supporting Information, S2). However, the presence and shifting of additional bands were observed. These irreproducible bands could be attributed to signal noise or some minor structural changes caused by a denaturation of the biomolecule when exposed to laser heat. Overall, the first two steps of the functionalization of AuNPs paper show a reasonably good SERS reproducibility.

Biotinylated anti-rabbit IgG, whose structure predominantly consists of  $\beta$ -sheet (47%),  $\alpha$ -helices, (7%) with the remaining molecule consisting of turns and coils [18], was then adsorbed onto the streptavidin-BAT/TEG functionalized AuNPs paper. The characteristic SERS bands of the antibody rabbit IgG were observed (Figure 16) [19–21]. The predominant  $\beta$ -sheet structure of IgG was identified by

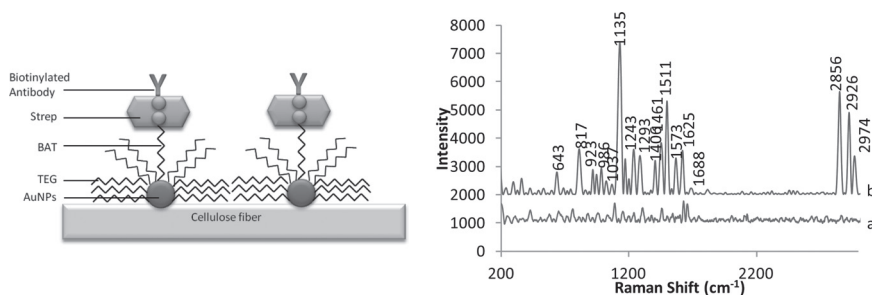


**Figure 16.** Left: Schematic diagram of biotinylated antibody-Strep-BAT/TEG functionalized AuNPs on paper. Right: SERS spectra of (a) biotinylated antibody on AuNPs paper and (b) biotinylated antibody-Strep-BAT/TEG functionalized AuNPs paper.

the characteristic amide III band around  $1243\text{ cm}^{-1}$  and a higher intensity band at  $1625\text{ cm}^{-1}$  in the amide I region.  $\alpha$ -helix structure was represented by the amide III band at  $1293\text{ cm}^{-1}$ . The other vibration bands generally associated with protein structures are assigned as follows:  $\nu(\text{C-H})$  around  $2856\text{ cm}^{-1}$  to  $2974\text{ cm}^{-1}$ ,  $\rho(\text{CH}_2)$  band was observed around  $1461\text{ cm}^{-1}$ . The bands related to tyrosine were observed around  $817\text{ cm}^{-1}$  and  $643\text{ cm}^{-1}$ . Trp residue bands were observed around  $1573\text{ cm}^{-1}$  and  $1406\text{ cm}^{-1}$  [19–20]. The bands in the region  $923\text{ cm}^{-1}$  could be assigned to  $\rho(\text{CH}_2)$  and the ones around  $986\text{ cm}^{-1}$  to  $\rho(\text{CH}_3)$  vibrations. Backbone skeletal  $\nu(\text{C-C})$  vibration bands were also observed in the region of  $1135\text{ cm}^{-1}$  to  $1037\text{ cm}^{-1}$ . The characteristic bands of the antibody show a good reproducibility with small variations in their Raman shift ( $\pm 10\text{--}20\text{ cm}^{-1}$ ) and intensity ( $\pm 20\text{--}30\%$ ).

After validating the reliability and reproducibility of the SERS spectrum of the antibody, the rabbit IgG antigen was adsorbed onto the antibody-streptavidin-BAT/TEG functionalized AuNPs paper. The combination of an antibody with its relative antigen is generally considered as a reversible bimolecular reaction with negligible changes in free energy. The antibody typically binds the antigen with very weak bonds as for example Van der Waals forces, Coulombic interactions between groups of opposite charges and hydrogen bonds [22]. Since all these interactions are very weak, the immunocomplex stability should depend on the simultaneous formation of many very weak bonds. Due to the weakness of the interaction, the mean secondary structure of antigen and antibody does not change significantly [22]. However, some interesting and new spectral features assumed to be produced by antibody-antigen interaction can still be observed (Figure 17). Comparing Figure 16 and Figure 17, the amide III region ( $1243\text{ cm}^{-1}$  and  $1625\text{ cm}^{-1}$ ) corresponding to the  $\beta$ -sheet structure reduced in intensity with a small shift. Moreover, the Amide III band at  $1293\text{ cm}^{-1}$  associated with  $\alpha$ -helix slightly shifted to the left

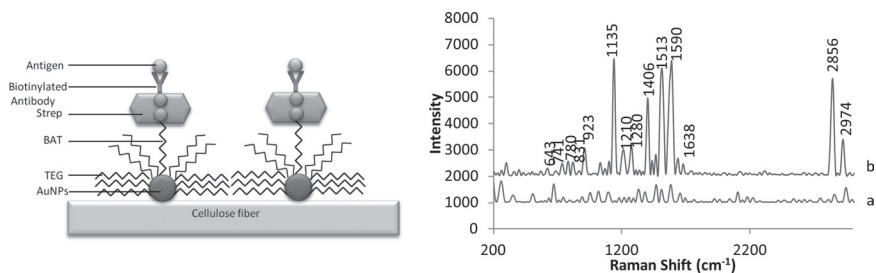


**Figure 17.** Left: Schematic diagram of antigen-biotinylated antibody-Strep-BAT/TEG functionalized AuNPs on paper. Right: SERS spectra of (a) antigen on AuNPs paper and (b) antigen-biotinylated antibody-Strep-BAT/TEG functionalized AuNPs paper.

to 1280 cm<sup>-1</sup>. An important observation from the antibody-antigen interaction spectra is the predominant presence of Trp residue bands around 1590 cm<sup>-1</sup> and 1406 cm<sup>-1</sup>. A few new bands at 741 cm<sup>-1</sup>, 780 cm<sup>-1</sup> and 831 cm<sup>-1</sup> associated with tyrosine residue were also observed [19]. They were all reproducible from measurement to measurement (Supporting Information, S2), providing a reliable means of detecting the presence of antigen. These observations are spectroscopic evidences for the antigen-antibody interaction as tryptophan and tyrosine residues are known to be involved in antibody-antigen binding [23–24].

The SERS sensitivity of the AuNPs paper was quantified. The AuNPs papers functionalized step by step with BAT/TEG, strep and antibody were exposed to different concentrations of antigen solutions and their SERS spectra were measured (Figure 18). The SERS intensity was increased as the function of

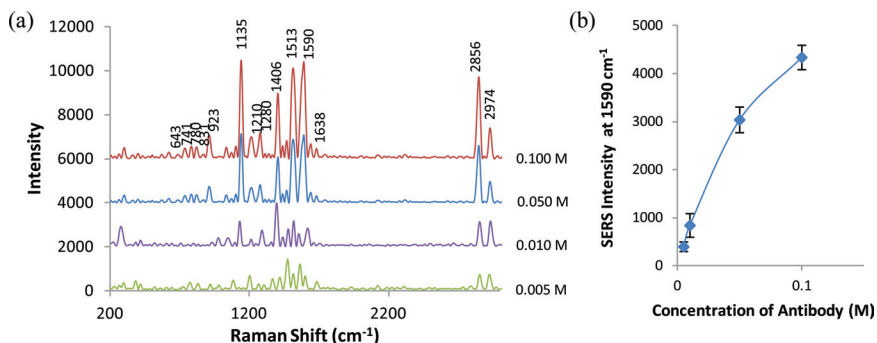


**Figure 18.** (a) SERS spectra of antigen-biotinylated antibody-Strep-BAT/TEG functionalized AuNPs paper exposed to different concentration of antigen. (b) SERS intensity of different concentration of antigen on functionalized AuNPs paper at 1590 cm<sup>-1</sup> band.

the concentration. The sensitivity of AuNPs paper could distinguish changes in protein conformation upon relaxation on a surface.

#### **4 CONCLUSION**

Gold nanoparticles (AuNPs) treated paper was investigated as a generic platform for low cost bio-diagnostic using Surface Enhanced Raman Scattering (SERS). In the first part of this study, the SERS sensitivity of AuNPs treated paper was quantified and optimized with 4-ATP, a model Raman molecule. A surface coverage of AuNPs ranging from 1.8 to 22.1% was achieved on paper as the concentration of AuNP solution, with which paper was treated, was increased. The SERS efficiency factor increased with the surface coverage and aggregate size of AuNPs on paper. To maximize the spatial density of SERS hotspots for optimized SERS signals, the aggregation size and surface coverage of AuNPs on paper was controlled by pre-treating paper with a series of cationic polyacrylamide (CPAM) solutions. Higher surface coverage and aggregation of AuNPs on paper was achieved with the more concentrated polymer solutions, with CPAM of higher charge density and higher molecular weight. A more uniform coverage of AuNPs was formed on CPAM treated paper than on the bare paper. A surface coverage of AuNPs up to 80% with average AuNP aggregates up to 60 nm on paper was achieved. The resulting Raman EF was almost an order of magnitude higher and more reproducible than that from the untreated AuNPs paper, at a constant concentration of AuNPs suspension.

The second part of this study analysed the selectivity of AuNPs treated paper as a SERS bio-diagnostic platform for quantitative and qualitative detection of a specific antibody interacting with its antigen. The AuNPs preadsorbed on paper were functionalized step by step by using streptavidin/biotin assemblies to detect antibody-antigen interactions. SERS spectra with specific features were obtained at each of the functionalization steps of biomolecules on the AuNPs-paper, confirming the capability for qualitative detection. Predominant tryptophan and tyrosine residue bands were detected upon antigen binding, confirming the presence of antigen. The shifts of Raman band associated with the  $\alpha$ -helix and  $\beta$ -sheet structure also indicated the modification of the local structure of antibody upon interaction with its specific antigen. Reproducible spectral features varying in intensity were observed as AuNPs-papers were subjected to different concentrations of antigen solutions, indicating good qualitative detection of biomolecules.

AuNPs paper is a promising generic platform for the specific detection of trace amounts of antibody in complex environments by SERS technology. This simply involves adsorbing a thiol capped antigen on the AuNP paper followed by a

simple blocking step. An alternative functionalization is to rely on streptavidin-biotin coupling of the antigen on the AuNPs. The method is cost-effective, robust and convenient as no fluorescent labelling is required. The detection of low concentration biomolecules in clinical, forensic, industrial, and environmental laboratories are prospective applications of the technology.

## 5 ACKNOWLEDGEMENT

Thanks to Dr. T. Williams, Monash Centre for Electron Microscopy (MCEM), for FESEM technical expertise and F. Shanks from Monash Molecular Spectroscopy and Centre for Biospectroscopy for Raman technical advice. The financial supports from the ARC Linkage LP0989823 and Visy, Amcor, SCA, Norske Skog, Australian Paper, the Australian Pulp and Paper Institute and Monash University are all acknowledged. Many thanks to AQUA+TECH for providing polymer and technical expertise.

## 6 REFERENCES

1. Al-Tamimi, M., W. Shen, R. Zeineddine, H. Tran, and G. Garnier, *Validation of Paper-Based Assay for Rapid Blood Typing*. *Analytical Chemistry*, 2011. **84**(3): p. 1661–1668.
2. Khan, M.S., G. Thouas, W. Shen, G. Whyte, and G. Garnier, *Paper Diagnostic for Instantaneous Blood Typing*. *Analytical Chemistry*, 2010. **82**(10): p. 4158–4164.
3. Pelton, R., *Bioactive paper provides a low-cost platform for diagnostics*. *TrAC Trends in Analytical Chemistry*, 2009. **28**(8): p. 925–942.
4. Then, W.L. and G. Garnier, *Paper Biodiagnostics in Biomedicine*. *Analytical Chemistry*, 2013. **Submitted**.
5. Li, M., J. Tian, M. Al-Tamimi, and W. Shen, *Paper-Based Blood Typing Device That Reports Patient's Blood Type "in Writing"*. *Angewandte Chemie International Edition*, 2012. **51**(22): p. 5497–5501.
6. Ngo, Y.H., D. Li, G.P. Simon, and G. Garnier, *Paper surfaces functionalized by nanoparticles*. *Advances in Colloid and Interface Science*, 2011. **163**(1): p. 23–38.
7. Ngo, Y.H., D. Li, G.P. Simon, and G. Garnier, *Gold Nanoparticle–Paper as a Three-Dimensional Surface Enhanced Raman Scattering Substrate*. *Langmuir*, 2012. **28**(23): p. 8782–8790.
8. Ngo, Y.H., D. Li, G.P. Simon, and G. Garnier, *Effect of cationic polyacrylamides on the aggregation and SERS performance of gold nanoparticles-treated paper*. *Journal of Colloid and Interface Science*, 2013. **392**(0): p. 237–246.
9. Turkevich, J., P.C. Stevenson, and J. Hillier, *A study of the nucleation and growth processes in the synthesis of colloidal gold*. *Discussions of the Faraday Society* 1951. **11**: p. 55–75.

10. Camargo, P.H.C., L. Au, M. Rycenga, W. Li, and Y. Xia, *Measuring the SERS enhancement factors of dimers with different structures constructed from silver nanocubes*. Chemical Physics Letters, 2010. **484**(4–6): p. 304–308.
11. Hu, X., T. Wang, L. Wang, and S. Dong, *Surface-Enhanced Raman Scattering of 4-Aminothiophenol Self-Assembled Monolayers in Sandwich Structure with Nanoparticle Shape Dependence: Off-Surface Plasmon Resonance Condition*. Journal of Physical Chemistry C, 2007. **111**(19): p. 6962–6969.
12. Peacock, A.C., A. Amezcua-Correa, J. Yang, P.J.A. Sazio, and S.M. Howdle, *Highly efficient surface enhanced Raman scattering using microstructured optical fibers with enhanced plasmonic interactions*. Applied Physics Letters, 2008. **92**(14).
13. Hu, X., T. Wang, L. Wang, and S. Dong, *Surface-Enhanced Raman Scattering of 4-Aminothiophenol Self-Assembled Monolayers in Sandwich Structure with Nanoparticle Shape Dependence: Off-Surface Plasmon Resonance Condition*. Journal of Physical Chemistry C, 2007. **111**(19): p. 6962–6969.
14. Oh, M.K., S. Yun, S.K. Kim, and S. Park, *Effect of layer structures of gold nanoparticle films on surface enhanced Raman scattering*. Analytica Chimica Acta, 2009. **649**(1): p. 111–116.
15. Michaels, A.M., Jiang, and L. Brus, *Ag Nanocrystal Junctions as the Site for Surface-Enhanced Raman Scattering of Single Rhodamine 6G Molecules*. The Journal of Physical Chemistry B, 2000. **104**(50): p. 11965–11971.
16. He, J., P. Zhang, J. Gong, and Z. Nie, *Facile synthesis of functional Au nanopatches and nanocups*. Chemical Communications, 2012. **48**(59): p. 7344–7346.
17. Galarreta, B.C., P.R. Norton, and F.o. Laguné-Labarhet, *SERS Detection of Streptavidin/Biotin Monolayer Assemblies†*. Langmuir, 2011. **27**(4): p. 1494–498.
18. Sjöholm, I., *Protein A from Staphylococcus aureus*. European Journal of Biochemistry, 1975. **51**(1): p. 55–61.
19. Naumann, D., *FT-INFRARED AND FT-RAMAN SPECTROSCOPY IN BIOMEDICAL RESEARCH*. Applied Spectroscopy Reviews, 2001. **36**(2–3): p. 239–298.
20. Kengne-Momo, R.P., P. Daniel, F. Lagarde, Y.L. Jeyachandran, J.F. Pilard, M.J. Durand-Thouand, and G. Thouand, *Protein Interactions Investigated by the Raman Spectroscopy for Biosensor Applications*. International Journal of Spectroscopy, 2012. **2012**: p. 7.
21. Chou, I.H., M. Benford, H.T. Beier, G.L. Coté, M. Wang, N. Jing, J. Kameoka, and T.A. Good, *Nanofluidic biosensing for beta-amyloid detection using surface enhanced Raman spectroscopy*. Nano Letters, 2008. **8**(6): p. 1729–1735.
22. Matharu, Z., A.J. Bandodkar, V. Gupta, and B.D. Malhotra, *Fundamentals and application of ordered molecular assemblies to affinity biosensing*. Chemical Society Reviews, 2012. **41**(3): p. 1363–1402.
23. Davies, D.R. and G.H. Cohen, *Interactions of protein antigens with antibodies*. Proceedings of the National Academy of Sciences, 1996. **93**(1): p. 7–12.
24. Ohno, S., N. Mori, and T. Matsunaga, *Antigen-Binding Specificities of Antibodies are Primarily Determined by Seven Residues of VH*. Proceedings of the National Academy of Sciences of the United States of America, 1985. **82**(9): p. 2945–2949.

## Transcription of Discussion

# GOLD NANOPARTICLES PAPER AS SURFACE ENHANCED RAMAN SCATTERING (SERS) PLATFORM FOR BIO-DIAGNOSTIC APPLICATIONS

*Ying Hui Ngo, Whui Lyn Then and Gil Garnier*

BioPRIA, Australian Pulp and Paper Institute (APPI), Department of Chemical Engineering, Monash University, Clayton, VIC 3800, Australia.

*Anders Åström*      Aylesford Newsprint (from the chair)

First one comment, I guess if you have gold in your paper there won't be any question about not getting good recycling rates. How do you expect the paper to be recovered?

*Gil Garnier*

Probably recovered, or yes, perhaps flushed, but it won't be recycled!

*Bob Pelton*      McMaster University

I believe SERS is currently used for antibody reporting in conventional biochemistry labs. Can you tell us what the conventional substrates are, and how do your paper substrates compare with the conventional substrates?

*Gil Garnier*

Yes, basically, it is used wet, in liquid. That means you have a solution, you have a detector that you put into your solution; that is how it is used most of the time. The alternative is silicon wafers, but that process is fairly expensive, and is, we believe, much less flexible than using paper. With paper you can combine it with micro-fluidics; you can quantify if you need to separate components.